Circadian key component CLOCK/BMAL1 interferes with segmentation clock in mouse embryonic organoids

Yasuhiro Umemura[a], **Nobuya Koike**[a], **Yoshiki Tsuchiya**[a], **Hitomi Watanabe**[b], **Gen Kondoh**[b], **Ryoichiro Kageyama**[c], and **Kazuhiro Yagita**[a,1]

[a]Department of Physiology and Systems Bioscience, Kyoto Prefectural University of Medicine, Kyoto 602-8566, Japan; [b]Laboratory of Integrative Biological Science, Institute for Frontier Life and Medical Sciences, Kyoto University, Kyoto 606-8501, Japan; and [c]Laboratory of Growth Regulation System, Institute for Frontier Life and Medical Sciences, Kyoto University, Kyoto 606-8507, Japan

Edited by Joseph Takahashi, HHMI and Department of Neuroscience, The University of Texas Southwestern Medical Center, Dallas, TX; received July 30, 2021; accepted November 16, 2021

In mammals, circadian clocks are strictly suppressed during early embryonic stages, as well as in pluripotent stem cells, by the lack of CLOCK/BMAL1-mediated circadian feedback loops. During ontogenesis, the innate circadian clocks emerge gradually at a late developmental stage, and with these, the circadian temporal order is invested in each cell level throughout a body. Meanwhile, in the early developmental stage, a segmented body plan is essential for an intact developmental process, and somitogenesis is controlled by another cell-autonomous oscillator, the segmentation clock, in the posterior presomitic mesoderm (PSM). In the present study, focusing upon the interaction between circadian key components and the segmentation clock, we investigated the effect of the CLOCK/BMAL1 on the segmentation clock *Hes7* oscillation, revealing that the expression of functional CLOCK/BMAL1 severely interferes with the ultradian rhythm of segmentation clock in induced PSM and gastruloids. RNA sequencing analysis implied that the premature expression of CLOCK/BMAL1 affects the *Hes7* transcription and its regulatory pathways. These results suggest that the suppression of CLOCK/BMAL1-mediated transcriptional regulation during the somitogenesis may be inevitable for intact mammalian development.

circadian clock | segmentation clock | CLOCK | BMAL1 | gastruloid

The circadian clock is the cell-autonomous time-keeping system generating the orderly regulated various physiological functions, which enables cells, organs, and systems to adapt to the cyclic environment of the rotating Earth (1–5). The core architecture of the circadian molecular clock consists of negative transcriptional/translational feedback loops (TTFLs) composed of a set of circadian clock genes, including *Bmal1*, *Clock*, *Period* (*Per1*, *2*, *3*), and *Cryptochrome* (*Cry1*, *2*), functioning under the control of E-box elements (2, 6). The kernel of circadian TTFLs is composed of heterodimerized CLOCK/BMAL1 key transcriptional factors that positively regulate the circadian output genes, as well as *Per* and *Cry* genes via E-box. PERs and CRYs inhibit CLOCK/BMAL1 transcriptional activity, and the negative feedback loops between these genes generate oscillations of ∼24 h.

In mammalian development, it has been demonstrated that early embryos and pluripotent stem cells have no apparent circadian molecular oscillations (7–11), whereas the innate circadian clock develops during ontogenesis and is established at a late developmental stage (12–15). Regarding the mechanisms regulating circadian clock development, using an in vitro model of embryonic stem cell (ESC) differentiation and mouse embryos, it was shown that prolonged posttranscriptional mechanisms, such as suppressed translation of CLOCK protein and predominant cytoplasmic localization of PER proteins, inhibit the establishment of the circadian TTFL cycle (16–18). Although it was revealed that the multiple mechanisms strictly suppress the circadian molecular clock in the undifferentiated cells and early-stage embryos, the biological and physiological significance of the delayed emergence of circadian clock oscillation in mammalian embryos has been unknown.

In the early developmental stages, a segmented body plan is essential for an intact developmental process. Somitogenesis is related to another cell-autonomous oscillator, the segmentation clock, in the posterior presomitic mesoderm (PSM) (19, 20). The mouse segmentation clock is underlain by a negative feedback loop involving *Hes7* oscillation (21, 22). HES7 is a key transcriptional factor that represses its own expression and oscillates through a negative feedback loop in a period of 2–3 h in mouse and 4–5 h in humans. The NOTCH, WNT, and fibroblast growth factor signaling pathways are involved in the regulation of the *Hes7* oscillator and its intercellular synchronization (20). In mammals, however, there is a lack of knowledge about the sequential emergence of two different types of rhythmic phenomena and their biological significance during development.

In this study, focusing on the relationship between the circadian clock and segmentation clock, we investigated the effect of the premature expression of CLOCK/BMAL1 on the segmentation clock oscillation and revealed severe interference with the ultradian rhythm of segmentation clock in induced PSM (iPSM) and gastruloids. RNA sequencing analysis implied that CLOCK/BMAL1 affects the *Hes7* transcription and its regulatory pathways. These findings highlight that the suppression of functional CLOCK/BMAL1, which leads to arrest of

Significance

Although the circadian clock is essential for regulating the temporal order of physiological functions, circadian oscillation is strictly suppressed in the early-to-mid–stage embryos in mammalian developmental process. The biological significance controlling the suppression of the circadian clock and its delayed emergence in mammalian embryos has been unknown. Here, we show that the premature expression of the functional circadian components CLOCK/BMAL1 in mouse induced presomitic mesoderm and gastruloids can interfere with the segmentation clock *Hes7* oscillation and somitogenesis through the *Hes7* transcription and its regulatory pathways. This suggests that the CLOCK/BMAL1 function may need to be suppressed during somitogenesis.

Author contributions: Y.U. and K.Y. designed research; Y.U., Y.T., H.W., G.K., and K.Y. performed research; Y.U., N.K., Y.T., R.K., and K.Y. analyzed data; and Y.U., N.K., and K.Y. wrote the paper.

The authors declare no competing interest.

This article is a PNAS Direct Submission.

[1]To whom correspondence may be addressed. Email: kyagita@koto.kpu-m.ac.jp.

This article contains supporting information online at http://www.pnas.org/lookup/suppl/doi:10.1073/pnas.2114083119/-/DCSupplemental.

Published December 20, 2021.

DEVELOPMENTAL BIOLOGY

the circadian clock oscillation, during the early- to mid-developmental stage may be inevitable for the intact process of mammalian embryogenesis.

Results

A Circadian Clock Gene, *Per1*, and a Segmentation Clock Gene, *Hes7*, Are Adjacent Genes in the Mammalian Genome. In mammals, the temporal relationship between the segmentation clock and circadian clock appears to be mutually exclusive (*SI Appendix*, Fig. S1) (12–15, 19, 20). To explore the functional interaction between these two biological rhythms with different frequencies during the developmental process, we focused on the genomic architecture of genes comprising circadian and segmentation clocks, respectively. Intriguingly, one of the core circadian clock genes, *Per1*, is physically adjacent to an essential component of the segmentation clock, *Hes7*, in a genomic region conserved in higher vertebrates, including mice and humans. The *Per1* homolog *Per2* is adjacent to the *Hes7* homolog *Hes6* in the genome (Fig. 1*A*). *Hes6* is highly expressed in the nervous system and promotes neural differentiation (23). On the other hand, since *Hes7* exhibits the essential characteristics of a segmentation clock (24) and neighboring genes can influence the expressions with each other during somitogenesis in zebrafish (25), we focused on the effect of the regulation mechanism of the circadian clock on segmentation clock oscillation. Therefore, we investigated the effect of the CLOCK/BMAL1-mediated activation of *Per1* transcription on the segmentation clock oscillation in iPSM, an in vitro recapitulating model of a segmentation clock, using ESCs carrying the *Hes7*-promoter–driven luciferase reporter (*pHes7-luc*) (26) (Fig. 1*B*). In the iPSM, the pluripotent markers have not yet been down-regulated sufficiently as previously reported (26), and the iPSM differentiated from $Per2^{Luc}$ ESCs showed no apparent circadian clock oscillation (*SI Appendix*, Fig. S2 *A*–*C*). In addition, the protein expression pattern of CLOCK, BMAL1, and PER1 in the iPSMs was quite similar to that in the undifferentiated ESCs (*SI Appendix*, Fig. S2 *D*–*F*) (16, 17), confirming that the circadian TTFL was not established and circadian clock oscillation was also strictly suppressed in the iPSM by the common inhibitory molecular mechanisms to the undifferentiated ESCs.

Because CLOCK/BMAL1 is a key transcription regulator of circadian TTFL and the expression of CLOCK protein is suppressed posttranscriptionally in iPSM as well as ESCs and early embryos (17), we established two ESC lines carrying both the doxycycline (Dox)-inducible *Clock* and *Bmal1* genes (Fig. 1*C* and *SI Appendix*, Fig. S3). In iPSM differentiated from ESCs, the expression of both *Clock*/*Bmal1* messenger RNA (mRNA) and CLOCK/BMAL1 proteins was confirmed after the addition of Dox (Fig. 1 *D* and *E*), and we found that overexpression of both *Clock* and *Bmal1* successfully activated the expression of core clock genes (Fig. 2*A*). As the dominant negative mutant of *Bmal1* (*Bmal1DN*) (27) coexpressed with *Clock* did not activate the *Per1*/*2* and *Cry1*/*2* genes, we concluded that CLOCK/BMAL1 specifically activated the expression of these clock genes via an E-box (Figs. 1 *C*–*E* and 2*A*). We then examined the expression of genes in *Hes7*, which is proximal to *Per1*, and *Hes6*, which is proximal to *Per2* in the genome. The expression of *Clock*/*Bmal1* induced by Dox in the iPSM up-regulated the expression of the *Hes7* and *Hes6* statistically significantly (Fig. 2*B*). Similarly, we also observed the up-regulation of *Hes7* and *Hes6* by *Clock*/*Bmal1* induction in the undifferentiated ESCs (*SI Appendix*, Fig. S4 *A* and *B*). These results indicate that the circadian components CLOCK/BMAL1 also affect the segmentation clock gene *Hes7* and the circadian clock gene *Per1*, as well as *Hes6* and *Per2*.

Inhibition of *Hes7* Ultradian Rhythm by CLOCK/BMAL1 in iPSM. We next performed a functional analysis using the in vitro recapitulation model of a segmentation clock oscillation in iPSM (26). The oscillations in bioluminescence from *pHes7-luc* reporters were observed using a photomultiplier tube device (PMT) and an electron multiplying CCD (EM-CCD) camera (Fig. 3*A*). We confirmed an oscillation of *Hes7*-promoter–driven bioluminescence with a period of ∼2.5–3 h in control iPSM with or without Dox using PMT and the EM-CCD camera (Fig. 3 *B* and *C* and *SI Appendix*, Figs. S5 and S6*A* and Movie S1). Traveling waves of *pHes7-luc* bioluminescence were observed, indicating that the segmentation clock oscillation in iPSM was successfully recapitulated, consistent with a previous report (26). Using this iPSM-based segmentation clock system, we investigated the effect of *Clock*/*Bmal1* expression on *Hes7*-promoter–driven oscillation. The expression of *Clock*/*Bmal1* genes (Dox+) resulted in defects of the oscillation in *Hes7* promoter activity, whereas *pHes7-luc* bioluminescence continued to oscillate with the periods of ∼2.5–3 h under Dox− conditions. Oscillation of the segmentation clock with periods of ∼2.5–3 h was observed even during the induction of *Clock*/*Bmal1DN* (Fig. 3*D* and *SI Appendix*, Fig. S5), indicating that the CLOCK/BMAL1-mediated mechanism interfered with the transcriptional oscillation of *Hes7*. A traveling wave of *Hes7* promoter activity disappeared with the expression of *Clock*/*Bmal1* (Fig. 3 *E* and *F*; *SI Appendix*, Fig. S6*B*; Movies S2 and S3), and Dox-dependent arrest of *pHes7-luc* traveling wave oscillating with a period of ∼2.5–3 h (Fig. 3 *G* and *H*; *SI Appendix*, Fig. S6 *C*–*E*; Movies S4 and S5) clearly demonstrated CLOCK/BMAL1-mediated interference with *Hes7*-driven segmentation clock oscillation in iPSM.

Interference with Somitogenesis-like Segmentation by Induction of CLOCK/BMAL1 in Gastruloids. In addition, to explore the effect of CLOCK/BMAL1 expression on somitogenesis, we established the ESC-derived embryonic organoids gastruloids, recapitulating an embryo-like organization, including a somitogenesis-like process in vitro (28) (Fig. 4*A*). The *pHes7-luc* bioluminescence represented a traveling wave accompanied by the formation of segment-like structures with anteroposterior polarity, in which the gastruloids were stained with stripes of a somite marker, *Uncx4.1*, by in situ hybridization (Fig. 4 *B*–*D*; Movie S6; *SI Appendix*, Fig. S7*A*). Only Dox treatment in control gastruloids induced no change in the *pHes7-luc* bioluminescence oscillation and somitogenesis-like process (Fig. 4 *E*–*G*; Movie S7; *SI Appendix*, Fig. S7*B*). The Dox-inducible *Clock*/*Bmal1* ESC line carrying *pHes7-luc* was differentiated in vitro into gastruloids and produced the somitogenesis-like process without Dox (Fig. 4 *H*–*J* and Movie S8 and *SI Appendix*, Fig. S7*C*). In contrast, the Dox-dependent induction of *Clock*/*Bmal1* expression in the gastruloids interrupted the *pHes7-luc* oscillation with a period of ∼2.5 h and disrupted the somitogenesis-like structures (Fig. 4 *K*–*M*; Movie S9; *SI Appendix*, Fig. S7 *D* and *E*). In gastruloids, the expression of *Clock*/*Bmal1* mRNA was confirmed after the addition of Dox (*SI Appendix*, Fig. S8). These results suggest that the premature expression of the circadian key transcriptional regulator CLOCK/BMAL1 critically interferes with not only *Hes7* oscillation but also somitogenesis.

CLOCK/BMAL1-Mediated Interference in the *Hes7* Regulatory Network. Next, to examine the perturbation mechanisms of the segmentation clock oscillation by the circadian components CLOCK/BMAL1, we analyzed the RNA sequencing (RNA-seq) data obtained from the total RNA of iPSM colonies. We extracted 509 up-regulated and 88 down-regulated differentially expressed genes (DEGs) after the induction of *Clock*/*Bma11* gene expression in iPSM colonies (Fig. 5*A*). A Kyoto Encyclopedia of Gene and Genomes (KEGG) pathway enrichment analysis for the DEGs indicated enrichment of the WNT, MAPK, and NOTCH signaling pathways related to *Hes7* oscillation (29) (Fig. 5*B*). Almost all other ranked pathways also included the WNT, MAPK, and NOTCH signaling pathway–related genes (Fig.

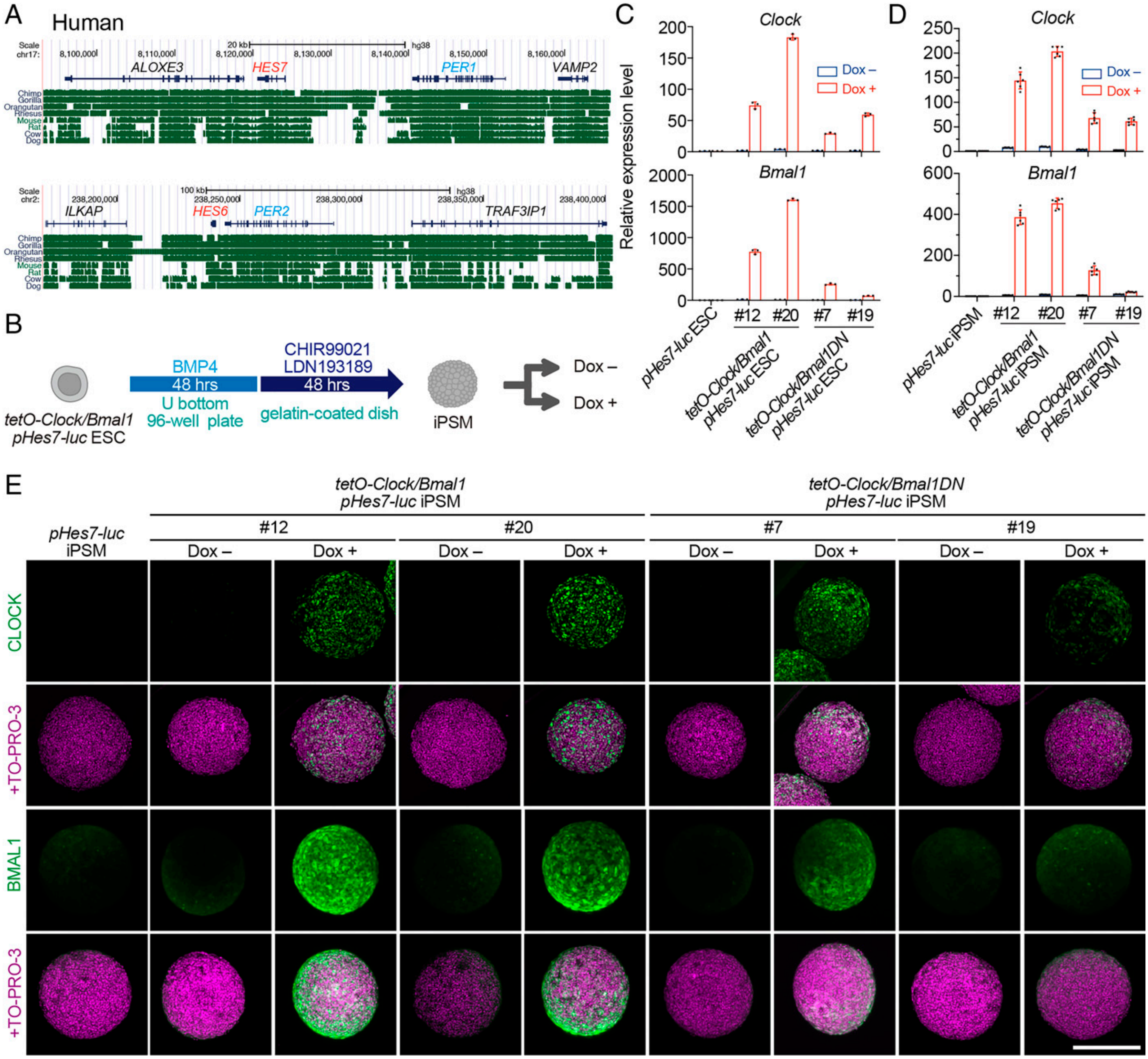

Fig. 1. Establishment of ESC lines carrying both the Dox-inducible *Clock* and *Bmal1* genes. (*A*) Human genomic locus of circadian clock genes, *PER1*, and the essential segmentation clock gene, *HES7*, are highly conserved in higher vertebrates. The *PER1* homolog *PER2* is also located adjacent to the *HES7* homolog *HES6* in the genome. (*B*) ESCs were differentiated into iPSM for 96 h in vitro, and then the iPSM colonies were treated with or without Dox. (*C*) qPCR of *Clock* and *Bmal1* mRNA in the indicated ESCs; 500 ng/mL Dox treatment for 6 h (red) or not (blue). Each number indicates clone number. Mean ± SD ($n = 3$ biological replicates). (*D*) qPCR of *Clock* and *Bmal1* mRNA in the indicated iPSM colonies; 1,000 ng/mL Dox treatment for 2 h (red) or not (blue); mean ± SD ($n = 6$ biological replicates). The average expression level of *pHes7-luc* ESCs or iPSM colonies without Dox was set to 1. (*E*) Representative maximum intensity projection of the immunostaining of iPSM colonies treated with 1,000 ng/mL Dox for 2 h or not. $n = 3$ biological replicates. (Scale bar, 250 μm.)

5*B*). Similarly, enrichment of the WNT, MAPK, and NOTCH signaling pathways by *Clock*/*Bmal1* induction was also observed in the undifferentiated ESCs (*SI Appendix*, Fig. S9 *A* and *B*). These results imply that the expression of CLOCK/BMAL1 affects the *Hes7*-related signaling pathways, which interferes with the feedback loop regulating *Hes7* oscillation. Intriguingly, in addition to *Hes7* gene expression, the expressions of *Aloxe3* and *Vamp2* in iPSM and ESCs, the other contiguous genes with *Per1*, were up-regulated with the induction of *Clock*/*Bmal1* expression, and this result was confirmed by quantitative RT-PCR (qRT-PCR) (Fig. 5 *C*–*E*; *SI Appendix*, Fig. S9 *C*–*E*), suggesting that forced expression of CLOCK/BMAL1 also may affect a wide region around the *Hes7* gene locus on the same chromosome. These results suggest that the premature expression of the circadian components CLOCK/BMAL1 may interfere with *Hes7* oscillation and somitogenesis by perturbing the *Hes7* expressions through indirect regulatory pathways (Fig. 5*F*). Because the loss of the *Hes7* ultradian expression rhythm in the mouse causes segmentation defects (22, 30), the oscillatory expression of *Hes7* is essential for mammalian development. Therefore, the results in this study suggest that it may be imperative that CLOCK/BMAL1 function is suppressed until the completion of segmentation and other related developmental events.

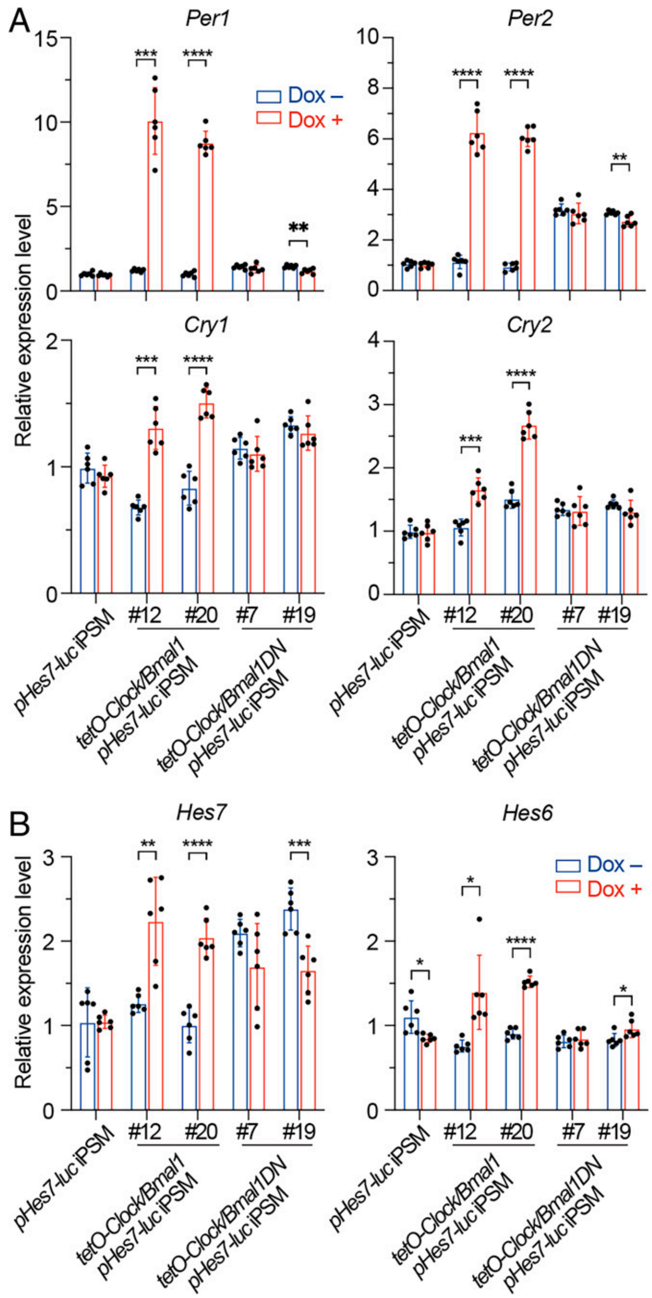

Fig. 2. CLOCK/BMAL1 expressions up-regulated not only circadian clock genes but also *Hes7* gene expression in the iPSM. (*A*, *B*) qPCR of core circadian clock genes (*A*) and *Hes7* or *Hes6* gene (*B*) in the indicated iPSM colonies; 1,000 ng/mL Dox treatment for 2 h (red) or not (blue); mean ± SD (n = 6 biological replicates). The average expression level of iPSM colonies without Dox was set to 1. Two-tailed t test, *$P < 0.05$, **$P < 0.01$, ***$P < 0.001$, ****$P < 0.0001$.

Discussion

Our present study showed that premature expression of circadian key components CLOCK/BMAL1 severely interferes with the ultradian rhythm of the segmentation clock in iPSM and gastruloids.

We have previously reported that during the early- to mid-developmental stage, there are multiple molecular mechanisms that underlie the strict suppression of circadian TTFLs, such as the posttranscriptional suppression of CLOCK protein (17, 18) and the exclusive cytoplasmic localization of PER proteins (16). Furthermore, we have also reported that the maternal circadian clock cannot entrain the fetus until the establishment of the fetal circadian clock itself (17). These results suggest that the circadian rhythm in mammalian embryos is rigorously suppressed by the multilayered inhibitory mechanisms during the early- to mid-developmental stage. During the multilayered suppression of circadian clock oscillation, the ultradian temporal oscillation of *Hes7* expression, the segmentation clock, proceeds and forms the spatial repetitive structure of somites.

In the present study, we investigated the effect of the CLOCK/BMAL1-mediated activation of *Per1* transcription on the segmentation clock oscillation by using the iPSM differentiated from ESCs. It was suggested that similar to the undifferentiated ESCs, circadian clock oscillation is suppressed in the iPSM by the common mechanisms to the ESCs and early embryos (see *SI Appendix*, Fig. S2). Recently, it was reported that hundreds of genes, including *Per1*, also oscillate in the same phase as *Hes7* ultradian rhythm in in vitro PSM of both mouse and humans (31), suggesting that *Per1* is deviated and free from the circadian gene regulatory mechanism of circadian TTFL. These findings are consistent with the previously reported observations indicating that the multilayered inhibitory mechanisms including posttranscriptional inhibition of CLOCK and the predominant cytoplasmic accumulation of PER1 do not allow the oscillation of circadian TTFL (17, 18). Interestingly, although the expression of BMAL1 protein was observed even in ESCs (17), the Dox-induced CLOCK sole expression in ESCs resulted in the only partial up-regulation of E-box–driven circadian clock genes (*SI Appendix*, Fig. S3), raising the possibility that the endogenously expressed BMAL1 might be posttranslationally modified to not function. Therefore, in this study, we used ESC lines carrying both the Dox-inducible *Clock* and *Bmal1* genes as a model system of premature expression of CLOCK/BMAL1 (see Fig. 1*C*).

It was suggested that the expression of CLOCK/BMAL1 affected the WNT, MAPK, and NOTCH signaling pathways related to *Hes7* oscillation in iPSM (see Fig. 5 *A* and *B*). In addition, the premature expression of CLOCK/BMAL1 resulted in not only the up-regulation of *Per1* expression but also the expression of *Hes7*, *Aloxe3*, and *Vamp2*, localized adjacently on the *Per1* genomic locus (see Figs. 2 *A* and *B* and 5 *C*–*E*; *SI Appendix*, Fig. S9 *C*–*E*). In the iPSM, the up-regulation of these genes' expression has already been induced after the 2-h Dox treatment (see Figs. 2 *A* and *B* and 5 *C*–*E*). Although the possibility of immediate transcriptional inductions by direct binding of CLOCK/BMAL1 to the promoters cannot be ruled out, considering that the *Per1* promoter harbors E-box elements with which CLOCK/BMAL1 heterodimer has a much higher affinity than the other genomic region (32), the immediate up-regulation of genes near *Per1* gene locus after the induction of CLOCK/BMAL1 expressions could be caused by the ripple effect (33). On the other hand, the bioluminescence from *Hes7*-promoter–driven luciferase reporters in the iPSM not only lost cycling but also decreased signal intensity ~2 h after the Dox addition (see Fig. 3*D*), suggesting that the expression of CLOCK/BMAL1 in the iPSM has also inhibitory effects on *Hes7* gene expression. Among the components involved in the *Hes7*-regulatory signaling pathways, expression of CLOCK/BMAL1 resulted in the induction of some negative regulators, such as the *Dusp* phosphatase family (34) in the MAPK signaling pathway, *Sfrp* in the WNT signaling pathway (35), and *Lfng* in the NOTCH signaling pathway (36) (see Fig. 5*B*). Therefore, the premature expression of CLOCK/BMAL1 first may up-regulate *Hes7* transcription and induce subsequent down-regulation of *Hes7* gene expression by the induction of the negative regulators in addition to the HES7 autoinhibition. Consequently, it was suggested that the premature expression of the circadian components CLOCK/BMAL1 may interfere with *Hes7* oscillation by perturbing the *Hes7* expression through various pathways.

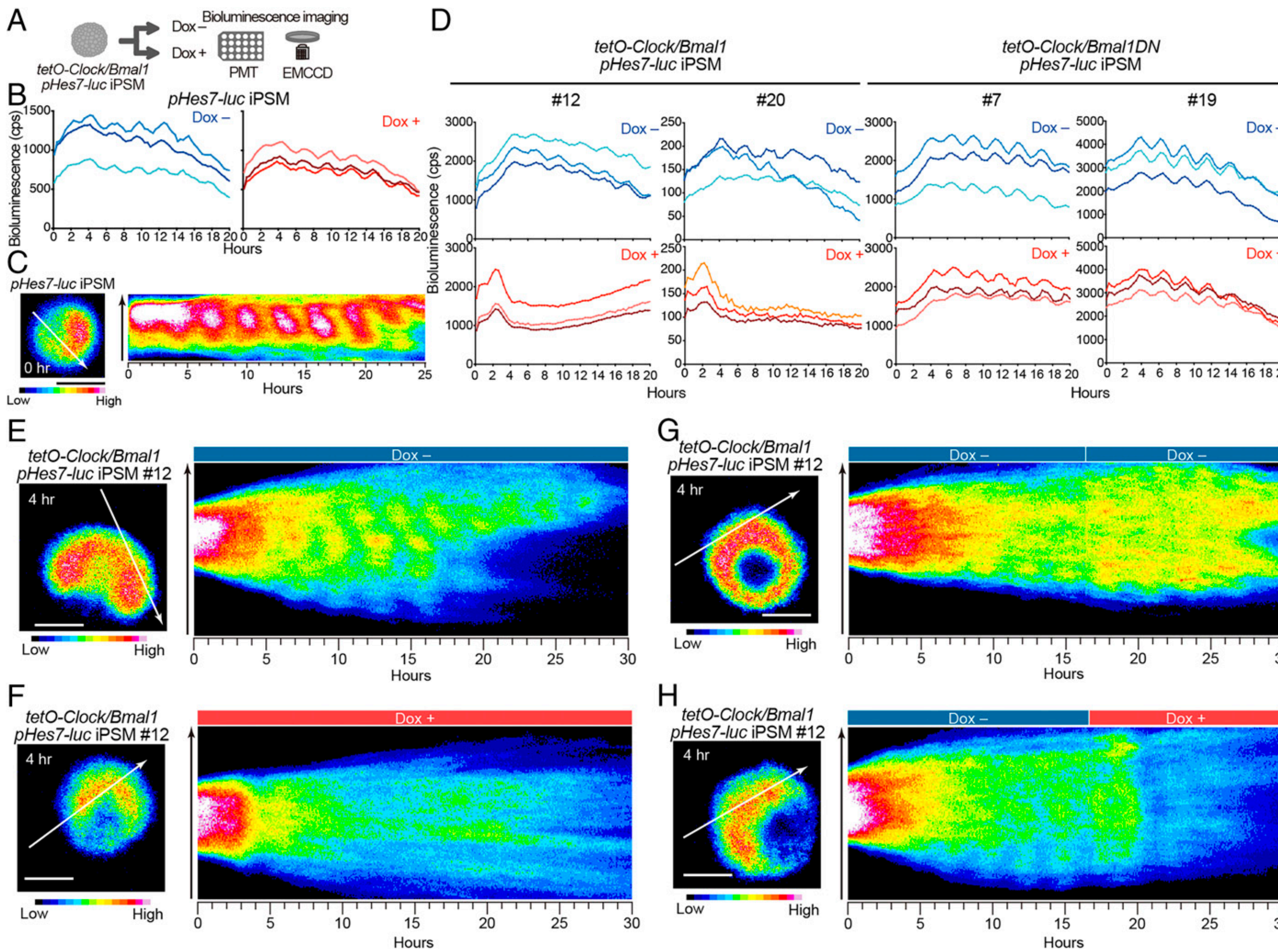

Fig. 3. CLOCK/BMAL1 expressions arrested the autonomous oscillations of *Hes7* in the iPSM colonies. (*A*) Bioluminescence of each Dox-inducible *Clock/Bmal1* or *Clock/Bmal1DN pHes7-luc* iPSM colony was observed using PMT or an EM-CCD camera without or with Dox. (*B*, *C*) Representative bioluminescence traces (*B*, n = 25 biological replicates) and live imaging (*C*, n = 3 biological replicates) of single *pHes7-luc* iPSM colony with or without Dox. The kymograph of the imaging along the arrow is shown. (*D*) Representative bioluminescence traces of the single indicated iPSM colony with and without 1,000 ng/mL Dox. n = 10–54 biological replicates. (*E*–*H*) Live imaging of the single *tetO-Clock/Bmal1 pHes7-luc* iPSM colony with and without Dox. Only medium or Dox-containing medium was added at the indicated time points at the final Dox concentration of 1,000 ng/mL (*G*, *H*). Each kymograph along the arrow is shown. (Scale bars, 250 μm.) n = 2–4 biological replicates.

In this study, we used a mouse embryonic organoid, gastruloids, as an in vitro recapitulation model of a somitogenesis-like process (28). The premature expression of CLOCK/BMAL1 in the gastruloids disrupted not only the *Hes7* oscillation but also the striped structure of the somite marker, *Uncx4.1* (see Fig. 4*M*). Because the RNA-seq analysis data showed that hundreds of genes were affected by the induction of CLOCK/BMAL1 (see Fig. 5*A*), the possibility cannot be denied that the premature expression of CLOCK/BMAL1 affects cell fates or characters. However, the posterior structure in the gastruloids was held even after the induction of CLOCK/BMAL1 and then continued to extend, concomitant with the decrease of *Hes7* bioluminescence signals and the arrest of the *Hes7* oscillation (see Fig. 4*K* and Movie S9), suggesting that the premature expression of CLOCK/BMAL1 interfered with the somitogenesis process by perturbing *Hes7* oscillation of the segmentation clock.

In vitro recapitulation of embryonic process using iPSM and gastruloids has differences such as no brain tissues compared with the in vivo process. However, the key regulators of somitogenesis we focus on in this study are expressed similarly between embryos and gastruloids using single-cell RNA-seq and spatial transcriptomics (28), and the in vitro recapitulation model enables us to analyze the *Hes7* oscillation in more detail using real-time imaging without maternal effects.

Our findings shown in this study indicated that CLOCK/BMAL1, key components regulating the circadian TTFL, affected and interfered with the segmentation clock. Considering that the transcriptional activation of CLOCK/BMAL1 is essential for the circadian regulatory networks, these results suggest that the strict suppression of circadian molecular oscillatory mechanisms in early-stage embryos may be inevitable for the intact developmental process in mammals. Therefore, this may be the biological and physiological significance of the delayed emergence of circadian clock oscillation observed in mammalian development.

Materials and Methods

Cell Culture. KY1.1 ESCs (7), referred to as ESCs in the text, and *Per2*^{Luc} ESCs (5, 37) were maintained as described previously (17). E14TG2a ESCs carrying *Hes7*-promoter–driven luciferase reporters (26), referred to as *pHes7-luc* ESCs in the text, were maintained without feeder cells in Dulbecco's Modified Eagle Medium (DMEM) (Nacalai) supplemented with 15% fetal bovine serum (HyClone), 2 mM L-glutamine (Nacalai), 1 mM nonessential amino acids (Nacalai), 100 μM StemSure 2-mercaptoethanol solution (Wako), 1 mM sodium pyruvate (Nacalai), 100 units/mL penicillin and streptomycin (Nacalai), 1,000 units/

https://doi.org/10.1073/pnas.2114083119

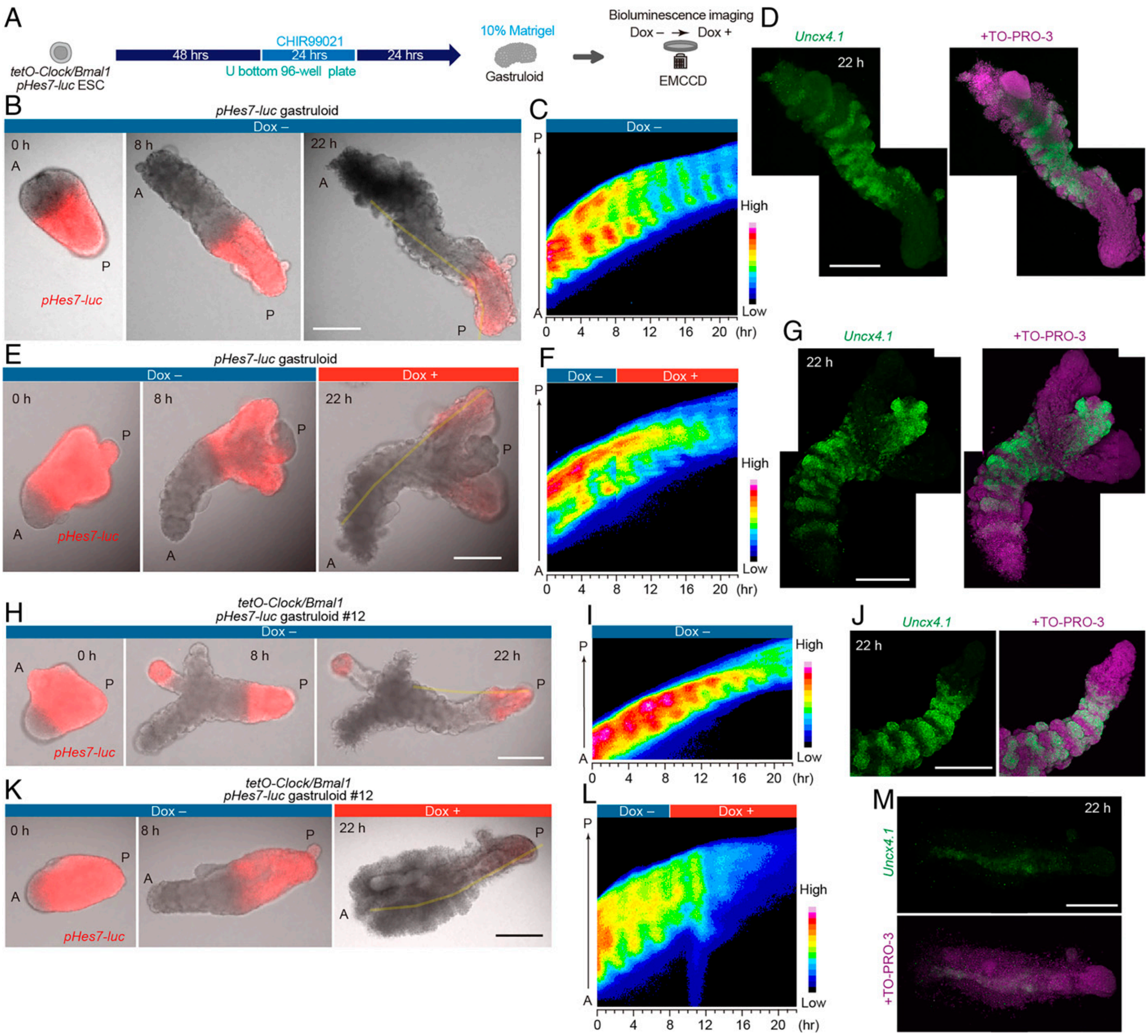

Fig. 4. CLOCK/BMAL1 expressions interfered with the autonomous oscillations of *Hes7* and somitogenesis-like process in the gastruloids. (*A*) Dox-inducible *Clock*/*Bmal1 pHes7-luc* ESCs were differentiated into gastruloids for 96 h in vitro, and then the gastruloids embedded in 10% Matrigel were treated with or without Dox. *pHes7-luc* bioluminescence was observed using an EM-CCD camera without or with Dox. (*B*–*M*) Time-lapse bioluminescence (red) and bright field imaging of the single *pHes7-luc* gastruloid or *tetO-Clock*/*Bmal1 pHes7-luc* gastruloid without and with Dox. Dox-containing medium was added at the indicated time points at the final Dox concentration of 1,000 ng/mL (*C*, *F*, *I*, and *L*). Each kymograph is shown along the yellow lines in *B*, *E*, *H*, and *K*. In situ hybridization of *Uncx4.1* in the gastruloids after the live cell imaging (*D*, *G*, *J*, *M*). (Scale bars, 250 μm.) $n = 3$ or 4 biological replicates.

mL leukemia inhibitory factor (Wako), 3 μM CHIR99021 (Wako or Tocris Biosciences), and 1 μM PD0325901 (Wako) with 5% CO_2 at 37 °C.

Transfection and Establishment of Cell Lines. ESCs stably expressing Dox-inducible *Clock*/*Bmal1* or *Clock*/*Bmal1DN* (I584X) were established as described previously (17). For *TetO-Clock*/*Bmal1* or *TetO-Clock*/*Bmal1DN* ESCs, KY1.1 ESCs or *pHes7-luc* ESCs were transfected using 10.5 μL of FuGENE 6 mixed with 1 μg of pCAG-PBase, 1 μg of PB-TET-Clock (17), 1 μg of PB-TET-Bmal1 or PB-TET-Bmal1DN (I584X), 1 μg of PB-CAG-rtTA Adv, and 0.5 μg of puromycin selection vector. The transfected cells were grown in a culture medium supplemented with 2 μg/mL puromycin for 2 d. The ESC colonies were picked and checked by qPCR after treatment with 500 ng/mL Dox. For PB-TET-Bmal1 and PB-TET-Bmal1DN (I584X), *Bmal1* complementary DNA (cDNA) and *Bmal1*DN (I584X) cDNA (27) were cloned into a PB-TET vector (38). For the *TetO-Clock Per2^{Luc}* ESCs, *Per2^{Luc}* ESCs were established as described previously (17).

Bioluminescence Imaging and Data Analysis. The iPSM colonies were differentiated from the *pHes7-luc* ESCs and *Per2^{Luc}* ESCs as described previously (26). The *Per2^{Luc}* ESCs were cultured without feeder cells in the ES medium containing 3 μM CHIRON99021 and 1 μM PD0325901 before in vitro differentiation. Bioluminescence imaging of single *pHes7-luc* iPSM colonies and *Per2^{Luc}* iPSM colonies was performed in gelatin-coated 24-well black plates or 35-mm dishes (27). DMEM was used that was supplemented with 15% knock-out serum replacement, 2 mM L-glutamine, 1 mM nonessential amino acids, 1 mM sodium pyruvate, 100 units/mL penicillin and streptomycin, 0.5% dimethyl sulfoxide (DMSO), 1 μM CHIR99021, and 0.1 μM LDN193189 (Sigma-Aldrich) containing 1 mM luciferin and 10 mM Hepes. For live imaging of single iPSM colonies using an EM-CCD camera, each iPSM colony was cultured on a fibronectin-coated glass base dish for 6 h, and images were acquired every 5 min with an exposure time of 5 or 10 s (control) and 2.5 s (*Clock*/*Bmal1* induction) under 5% CO_2 using an LV200 Bioluminescence Imaging System (Olympus). Periods were determined by measuring the average peak-to-peak intervals.

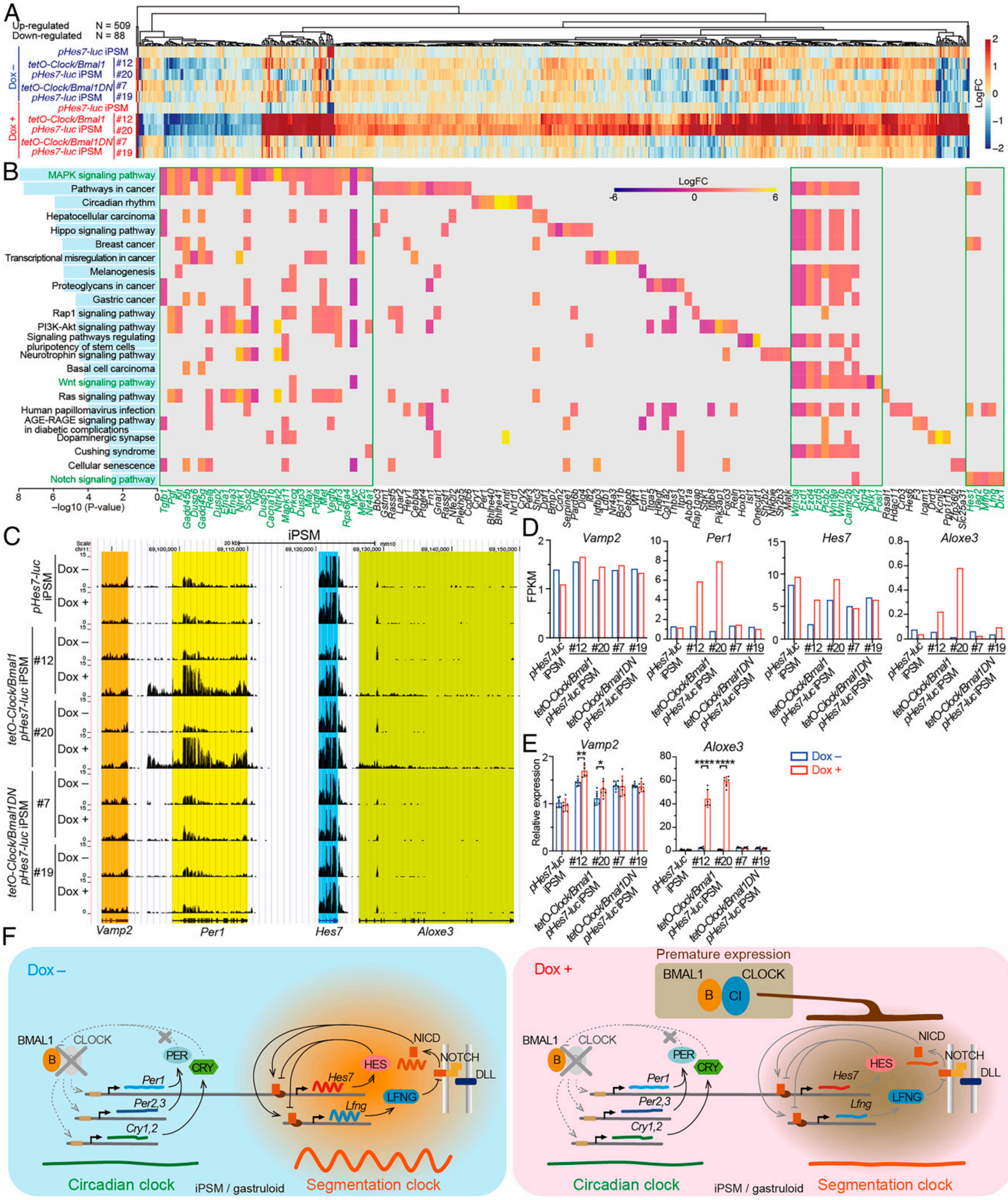

Fig. 5. CLOCK/BMAL1 expressions in the iPSM colonies may affect *Hes7*-related signaling pathways and up-regulate the expression of contiguous genes, *Per1*, *Hes7*, and *Aloxe3*. (*A*) Up-regulated and down-regulated DEGs in the indicated iPSM colonies treated with Dox. (*B*) KEGG pathway analysis of the DEGs. Each pathway was indicated with each transformed *P* value. The ranked pathways contained several common genes in the WNT, MAPK, and NOTCH signaling pathways. (*C*) University of California Santa Cruz (UCSC) genome browser views of RNA-seq data of the contiguous genes *Vamp2*, *Per1*, *Hes7*, and *Aloxe3*. The reads shown are normalized average reads per 10 million total reads in 10-bp bins. (*D*) mRNA expression of *Vamp2*, *Per1*, *Hes7*, and *Aloxe3* in the indicated iPSM colonies according to RNA-seq. (*E*) Validation of *Vamp2* and *Aloxe3* gene expression levels in the indicated iPSM colonies using qPCR. Colored boxes indicate 1,000 ng/mL Dox treatment for 2 h (red) or no treatment (blue). Mean ± SD (n = 6 biological replicates). The averaged expression level of *pHes7-luc* iPSM colonies without Dox was set to 1. Two-tailed t test, $*P < 0.05$, $**P < 0.01$, $****P < 0.0001$. (*F*) The premature expression of CLOCK/BMAL1 in the iPSM and gastruloids interfered with the segmentation clock oscillation and somitogenesis-like process. LogFC, Log fold change.

DEVELOPMENTAL BIOLOGY

Table 1. Forward and reverse primer sequences used

Gene	Forward or reverse	Sequence
Bmal1	F	CCACCTCAGAGCCATTGATACA
Bmal1	R	GAGCAGGTTTAGTTCCACTTTGTCT
Clock	F	ATTTCAGCGTTCCCATTTGA
Clock	R	TGCCAACAAATTTACCTCCAG
Per1	F	CCCAGCTTTACCTGCAGAAG
Per1	R	ATGGTCGAAAGGAAGCCTCT
Per2	F	CAGCACGCTGGCAACCTTGAAGTAT
Per2	R	CAGGGCTGGCTCTCACTGGACATTA
Cry1	F	TGAGGCAAGCAGACTGAATATTG
Cry1	R	CCTCTGTACCGGGAAAGCTG
Cry2	F	CTGGCGAGAAGGTAGAGTGG
Cry2	R	GACGCAGAATTAGCCTTTGC
Dbp	F	CGAAGAACGTCATGATGCAG
Dbp	R	GGTTCCCCAACATGCTAAGA
Hes6	F	CAACGAGAGTCTTCAGGAGCTGCG
Hes6	R	GCATGCACTGGATGTAGCCAGCAG
Hes7	F	GAGAGGACCAGGGACCAGA
Hes7	R	TTCGCTCCCTCAAGTAGCC
Vamp2	F	GAGCTGGATGACCGTGCAGATG
Vamp2	R	ATGGCGCAGATCACTCCCAAGA
Aloxe3	F	AAGCCCGCCAAGAATGTTATC
Aloxe3	R	CGGTTCCCAGAGTTGTCATCC
Actb	F	GGCTGTATTCCCCTCCATCG
Actb	R	CCAGTTGGTAACAATGCCATGT

F, forward; R, reverse.

Gastruloids were generated as described in a previous report (28). In total, 200–250 live cells were plated in 40 μL of N2B27 medium into each well of a U-bottomed non-tissue-culture–treated 96-well plate (Greinier 650185). After a 96-h cultivation, the gastruloids were embedded in 10% Matrigel (Corning 356231) containing 1 mM luciferin. For live imaging of single gastruloids, the images were acquired every 5 min with an exposure time of 3.5 s (*Clock*/*Bmal1* induction) or 10 s (control) under 5% CO_2 using the LV200 system. The videos were analyzed using the ImageJ software (39). Kymographs of the averaged bioluminescence intensity along the straight or segmented line of 5-pixel width were generated using the plug-in KymoResliceWide.

In Situ Hybridization. Hybridization chain reaction (HCR) v3 was performed as described previously (28, 40) using reagents procured from Molecular Instruments. *Uncx4.1* HCR probe (Accession NM_013702.3, hairpin B1) was labeled with Alexa Fluor 488.

qPCR. The iPSM colonies, ESCs, and gastruloids were washed with ice-cold phosphate buffered salts (PBS), and total RNA was extracted using Isogen reagent (Nippon Gene) or miRNeasy Mini Kits (Qiagen) according to the manufacturer's instructions. To remove the feeder cells from ESCs cultured on a feeder layer, the cells were treated with trypsin, and then the mixed cell populations were seeded on gelatin-coated dishes and incubated for 25 min at 37 °C three times in ESC medium. Nonattached ESCs were seeded in a gelatin-coated dish overnight and then treated with or without 500 ng/mL Dox for 6 h. The iPSM colonies and gastruloids were treated with or without 1,000 ng/mL Dox for 2 h. First-strand cDNAs were synthesized with 1,000 or 280 ng of total RNA using Moloney Murine Leukemia Virus (M-MLV) reverse transcriptase (Invitrogen) according to the manufacturer's instructions. qPCR analysis was performed using the StepOnePlus Real-Time PCR system (Applied Biosystems) and iTaq Universal SYBR Green Supermix (Bio-Rad Laboratories). Standard PCR amplification protocols were applied, followed by dissociation-curve analysis to confirm specificity. Transcription levels were normalized to the level of β-actin. The primer sequences listed in Table 1 were used.

RNA-Seq. The iPSM colonies and ESCs were washed with ice-cold PBS, and total RNA was extracted using miRNeasy Mini Kits (Qiagen) according to the manufacturer's instructions. Total RNA sequencing was conducted by Macrogen Japan on an Illumina NovaSeq 6000 with 101-bp paired-end reads. After trimming the adaptor sequences using Trimmomatic (41), the reads that mapped to ribosomal DNA (GenBank: BK000964.1) (42) were filtered out, and the sequence reads were mapped to the mouse genome (GRCm38/mm10) using spliced transcript alignment to a reference (STAR) (43), as described previously (16). To obtain reliable alignments, reads with a mapping quality of less than 10 were removed using sequence alignment/map (SAM) tools (44). The known canonical genes from GENCODE VM23 (45) were used for annotation, and the reads mapped to the gene bodies were quantified using Homer (46). The longest transcript for each gene was used for gene-level analysis. We assumed that a gene was expressed when there were more than 20 reads mapped on average to the gene body. Differential gene expression in the RNA-seq data were determined using DESeq2 with thresholds of false discovery rate (FDR) $<$ 0.05, fold change $>$ 1.5, and expression level cutoff $>$ 0.1 fragments per kilobase of exon per million mapped reads (FPKM) (47). WebGestalt was used for KEGG pathway enrichment analysis (48). In the RNA-seq data using iPSM colonies, the reads mapped in the promoter (chr11:69115096–69120473) and 3′-untranslated region (UTR) (chr11:69122995–69123324) of *Hes7* were filtered out to eliminate transcripts from the *pHes7-luc* reporter transgene. The heatmaps of gene expression and KEGG pathways were generated with R using the pheatmap and pathview packages, respectively.

Immunostaining. The iPSM colonies were fixed in cold methanol for 15 min at room temperature. The fixed iPSM was blocked with 1% bovine serum albumin (BSA) or 5% skim milk overnight at 4 °C and then incubated with anti-CLOCK mouse antibody (CLSP4) (49), anti-BMAL1 mouse antibody (MBL), anti-BMAL1 guinea pig antibody (16), or anti-PER1 rabbit antibody (AB2201, Millipore) overnight at 4 °C. After washing in 1% BSA, the iPSM colonies were incubated with a CF488A-conjugated donkey anti-mouse IgG (Nacalai), Cy3-conjugated goat anti-guinea pig IgG (Jackson), DyLight488-conjugated donkey anti-rabbit IgG (Jackson) for 2 h at 4 °C, and the nuclei were stained with TO-PRO-3 1:1,000 (Thermo Fisher Scientific) for 10–20 min. The iPSM colonies were washed in 1% BSA and observed using an LSM510 or 900 confocal laser scanning microscope (Zeiss).

Western Blot Analysis. Cells were lysed as described previously (17). The samples were resolved on sodium dodecyl sulfate–polyacrylamide gel electrophoresis (SDS-PAGE) using 7.5% gel (Bio-Rad), and the transferred polyvinylidine difluoride (PVDF) membranes were reacted with antibodies against CLOCK (1:3,000, CLSP4) (49), BMAL1 (1:5,000) (32), and β-actin (1:20,000, Sigma-Aldrich).

Data Availability. RNA sequence data are available at the NCBI Gene Expression Omnibus (https://www.ncbi.nlm.nih.gov/geo/query/acc.cgi?acc=GSE181295) (50). All other study data are included in the article and/or *SI Appendix*.

ACKNOWLEDGMENTS. We thank the Yagita laboratory members for technical assistance. This work was supported in part by grants-in-aid for scientific research from the Japan Society for the Promotion of Science to Y.U. (19K06679) and K.Y. (18H02600, 21H02664) and the Cooperative Research Program (Joint Usage/Research Center program) of the Institute for Frontier Life and Medical Sciences, Kyoto University (G.K. and K.Y.).

1. A. Balsalobre, F. Damiola, U. Schibler, A serum shock induces circadian gene expression in mammalian tissue culture cells. *Cell* **93**, 929–937 (1998).
2. J. S. Takahashi, Transcriptional architecture of the mammalian circadian clock. *Nat. Rev. Genet.* **18**, 164–179 (2017).
3. K. Yagita, F. Tamanini, G. T. van Der Horst, H. Okamura, Molecular mechanisms of the biological clock in cultured fibroblasts. *Science* **292**, 278–281 (2001).
4. S. Yamazaki *et al.*, Resetting central and peripheral circadian oscillators in transgenic rats. *Science* **288**, 682–685 (2000).
5. S. H. Yoo *et al.*, PERIOD2:LUCIFERASE real-time reporting of circadian dynamics reveals persistent circadian oscillations in mouse peripheral tissues. *Proc. Natl. Acad. Sci. U.S.A.* **101**, 5339–5346 (2004).
6. J. B. Hogenesch, H. R. Ueda, Understanding systems-level properties: Timely stories from the study of clocks. *Nat. Rev. Genet.* **12**, 407–416 (2011).
7. K. Yagita *et al.*, Development of the circadian oscillator during differentiation of mouse embryonic stem cells in vitro. *Proc. Natl. Acad. Sci. U.S.A.* **107**, 3846–3851 (2010).
8. J. D. Alvarez, D. Chen, E. Storer, A. Sehgal, Non-cyclic and developmental stage-specific expression of circadian clock proteins during murine spermatogenesis. *Biol. Reprod.* **69**, 81–91 (2003).
9. T. Amano *et al.*, Expression and functional analyses of circadian genes in mouse oocytes and preimplantation embryos: Cry1 is involved in the meiotic process independently of circadian clock regulation. *Biol. Reprod.* **80**, 473–483 (2009).
10. E. Kowalska, E. Moriggi, C. Bauer, C. Dibner, S. A. Brown, The circadian clock starts ticking at a developmentally early stage. *J. Biol. Rhythms* **25**, 442–449 (2010).
11. D. Morse, N. Cermakian, S. Brancorsini, M. Parvinen, P. Sassone-Corsi, No circadian rhythms in testis: Period1 expression is clock independent and developmentally regulated in the mouse. *Mol. Endocrinol.* **17**, 141–151 (2003).

12. F. C. Davis, R. A. Gorski, Development of hamster circadian rhythms: Role of the maternal suprachiasmatic nucleus. *J. Comp. Physiol. A Neuroethol. Sens. Neural Behav. Physiol.* **162**, 601–610 (1988).
13. C. Jud, U. Albrecht, Circadian rhythms in murine pups develop in absence of a functional maternal circadian clock. *J. Biol. Rhythms* **21**, 149–154 (2006).
14. S. M. Reppert, W. J. Schwartz, Maternal suprachiasmatic nuclei are necessary for maternal coordination of the developing circadian system. *J. Neurosci.* **6**, 2724–2729 (1986).
15. V. Carmona-Alcocer *et al.*, Ontogeny of circadian rhythms and synchrony in the suprachiasmatic nucleus. *J. Neurosci.* **38**, 1326–1334 (2018).
16. Y. Umemura *et al.*, Transcriptional program of Kpna2/Importin-α2 regulates cellular differentiation-coupled circadian clock development in mammalian cells. *Proc. Natl. Acad. Sci. U.S.A.* **111**, E5039–E5048 (2014).
17. Y. Umemura *et al.*, Involvement of posttranscriptional regulation of *Clock* in the emergence of circadian clock oscillation during mouse development. *Proc. Natl. Acad. Sci. U.S.A.* **114**, E7479–E7488 (2017).
18. Y. Umemura, I. Maki, Y. Tsuchiya, N. Koike, K. Yagita, Human circadian molecular oscillation development using induced pluripotent stem cells. *J. Biol. Rhythms* **34**, 525–532 (2019).
19. Y. Harima, I. Imayoshi, H. Shimojo, T. Kobayashi, R. Kageyama, The roles and mechanism of ultradian oscillatory expression of the mouse Hes genes. *Semin. Cell Dev. Biol.* **34**, 85–90 (2014).
20. A. Hubaud, O. Pourquié, Signalling dynamics in vertebrate segmentation. *Nat. Rev. Mol. Cell Biol.* **15**, 709–721 (2014).
21. Y. Bessho, H. Hirata, Y. Masamizu, R. Kageyama, Periodic repression by the bHLH factor Hes7 is an essential mechanism for the somite segmentation clock. *Genes Dev.* **17**, 1451–1456 (2003).
22. Y. Takashima, T. Ohtsuka, A. González, H. Miyachi, R. Kageyama, Intronic delay is essential for oscillatory expression in the segmentation clock. *Proc. Natl. Acad. Sci. U.S.A.* **108**, 3300–3305 (2011).
23. S. Bae, Y. Bessho, M. Hojo, R. Kageyama, The bHLH gene Hes6, an inhibitor of Hes1, promotes neuronal differentiation. *Development* **127**, 2933–2943 (2000).
24. Y. Bessho *et al.*, Dynamic expression and essential functions of Hes7 in somite segmentation. *Genes Dev.* **15**, 2642–2647 (2001).
25. O. Q. H. Zinani, K. Keseroğlu, A. Ay, E. M. Özbudak, Pairing of segmentation clock genes drives robust pattern formation. *Nature* **589**, 431–436 (2021).
26. M. Matsumiya, T. Tomita, K. Yoshioka-Kobayashi, A. Isomura, R. Kageyama, ES cell-derived presomitic mesoderm-like tissues for analysis of synchronized oscillations in the segmentation clock. *Development* **145**, dev156836 (2018).
27. Y. B. Kiyohara *et al.*, The BMAL1 C terminus regulates the circadian transcription feedback loop. *Proc. Natl. Acad. Sci. U.S.A.* **103**, 10074–10079 (2006).
28. S. C. van den Brink *et al.*, Single-cell and spatial transcriptomics reveal somitogenesis in gastruloids. *Nature* **582**, 405–409 (2020).
29. M. Kanehisa, S. Goto, KEGG: Kyoto encyclopedia of genes and genomes. *Nucleic Acids Res.* **28**, 27–30 (2000).
30. Y. Niwa *et al.*, The initiation and propagation of Hes7 oscillation are cooperatively regulated by Fgf and notch signaling in the somite segmentation clock. *Dev. Cell* **13**, 298–304 (2007).
31. M. Matsuda *et al.*, Recapitulating the human segmentation clock with pluripotent stem cells. *Nature* **580**, 124–129 (2020).
32. N. Koike *et al.*, Transcriptional architecture and chromatin landscape of the core circadian clock in mammals. *Science* **338**, 349–354 (2012).
33. M. Ebisuya, T. Yamamoto, M. Nakajima, E. Nishida, Ripples from neighbouring transcription. *Nat. Cell Biol.* **10**, 1106–1113 (2008).
34. D. M. Owens, S. M. Keyse, Differential regulation of MAP kinase signalling by dual-specificity protein phosphatases. *Oncogene* **26**, 3203–3213 (2007).
35. R. T. Moon, J. D. Brown, J. A. Yang-Snyder, J. R. Miller, Structurally related receptors and antagonists compete for secreted Wnt ligands. *Cell* **88**, 725–728 (1997).
36. J. K. Dale *et al.*, Periodic notch inhibition by lunatic fringe underlies the chick segmentation clock. *Nature* **421**, 275–278 (2003).
37. Z. Chen *et al.*, Identification of diverse modulators of central and peripheral circadian clocks by high-throughput chemical screening. *Proc. Natl. Acad. Sci. U.S.A.* **109**, 101–106 (2012).
38. Y. Inada *et al.*, Cell and tissue-autonomous development of the circadian clock in mouse embryos. *FEBS Lett.* **588**, 459–465 (2014).
39. C. A. Schneider, W. S. Rasband, K. W. Eliceiri, NIH Image to ImageJ: 25 years of image analysis. *Nat. Methods* **9**, 671–675 (2012).
40. H. M. T. Choi *et al.*, Third-generation *in situ* hybridization chain reaction: Multiplexed, quantitative, sensitive, versatile, robust. *Development* **145**, dev165753 (2018).
41. A. M. Bolger, M. Lohse, B. Usadel, Trimmomatic: A flexible trimmer for Illumina sequence data. *Bioinformatics* **30**, 2114–2120 (2014).
42. NCBI Resource Coordinators, Database resources of the National Center for Biotechnology Information. *Nucleic Acids Res.* **46**, D8–D13 (2018).
43. A. Dobin *et al.*, STAR: Ultrafast universal RNA-seq aligner. *Bioinformatics* **29**, 15–21 (2013).
44. H. Li *et al.*, 1000 Genome Project Data Processing Subgroup, The sequence alignment/map format and SAMtools. *Bioinformatics* **25**, 2078–2079 (2009).
45. A. Frankish *et al.*, GENCODE reference annotation for the human and mouse genomes. *Nucleic Acids Res.* **47**, D766–D773 (2019).
46. S. Heinz *et al.*, Simple combinations of lineage-determining transcription factors prime cis-regulatory elements required for macrophage and B cell identities. *Mol. Cell* **38**, 576–589 (2010).
47. M. I. Love, W. Huber, S. Anders, Moderated estimation of fold change and dispersion for RNA-seq data with DESeq2. *Genome Biol.* **15**, 550 (2014).
48. Y. Liao, J. Wang, E. J. Jaehnig, Z. Shi, B. Zhang, WebGestalt 2019: Gene set analysis toolkit with revamped UIs and APIs. *Nucleic Acids Res.* **47**, W199–W205 (2019).
49. H. Yoshitane *et al.*, Roles of CLOCK phosphorylation in suppression of E-box-dependent transcription. *Mol. Cell. Biol.* **29**, 3675–3686 (2009).
50. Y. Umemura, N. Koike, K. Yagita, Circadian key component CLOCK/BMAL1 interferes with segmentation clock in mouse embryonic organoids. NCBI Gene Expression Omnibus. https://www.ncbi.nlm.nih.gov/geo/query/acc.cgi?acc=GSE181295. Deposited 2 August 2021.